

HIGH SURFACE AREA MIXED METAL OXIDES AND HYDROXIDES

FEDERALLY SPONSORED RESEARCH/DEVELOPMENT PROGRAM

This invention was made with government support under Grant DAAD19-99-1-0228 awarded by the United States Army Research Office. The government has certain rights in the invention.

BACKGROUND OF THE INVENTION

Field of the Invention

The present invention is directed to multiple-component, highly reactive nanocrystalline compositions including at least two nanocrystalline materials selected from the oxides and hydroxides of the elements of Groups IIA, IIIA, IVA, the transition metals and the lanthanide series of the Periodic Table, wherein the materials are solidified and intimately intermingled on a molecular level. Such compositions exhibit very small average crystallite sizes and correspondingly large surface areas. A synthesis for such compositions also forms a part of the invention, along with methods of use thereof. Nanocrystalline aluminum oxides having BET surface areas of at least about 700 m²/g are also disclosed..

Description of the Prior Art

Considerable work has been done in the past in connection with the synthesis and use of various nanocrystalline (NC) metal oxides such as aluminum and magnesium oxides. Such materials have very high surface areas and some have been shown to be excellent adsorbents for a variety of target substances such as chlorinated hydrocarbons. NC metal oxides are often much more reactive than their conventionally or commercially made (CM) metal oxide counterparts. Nanocrystalline oxides have been prepared as single oxides or as composites with a core oxide and a coating of a second, different oxide. See, e.g., U.S. Patents Nos. 6,087,294, 6,057,488, 5,712,219, 6,045,925, 5,914,436, 5,759,939 and 5,712,219.

Mixed metal oxides also play an appreciable role in many areas of chemistry and physics. The unique electronic and magnetic properties obtained when combining two metals in an oxide

matrix have been well studied. However, the most common use for mixed metal oxides has been in the area of catalysis, and here they have found use both as the catalyst and as the support. Specifically, mixed metal oxides containing aluminum have found catalysis uses, such as:

- Destructive oxidation of methyl sulfide ($\text{CuO}/\text{Al}_2\text{O}_3$)
- Denitrogenation of heteroaromatic compounds ($\text{Mo}/\text{Al}_2\text{O}_3\text{-SiO}_2$)
- Isomerization of olefins, paraffins, and alkyl aromatics ($\text{Al}_2\text{O}_3/\text{SiO}_2$)
- Ammoxidation of 3-picoline ($\text{V}_2\text{O}_5/\text{Al}_2\text{O}_3\text{-SiO}_2$)
- Dimerization and oligomerization of olefins ($\text{NiO}/\text{Al}_2\text{O}_3\text{-SiO}_2$)
- Combustion of methane ($\text{Pd}/\text{Al}_2\text{O}_3\text{-SiO}_2$)

The mixed $\text{MgO}/\text{Al}_2\text{O}_3$ system has been studied by several research groups for many applications, including catalysis. In 1996 Abello, et al. studied Mo supported on $\text{MgO}/\text{Al}_2\text{O}_3$ for the oxidative dehydration of propane. Preparation of the catalyst was conducted by impregnating alumina with a solution of $\text{Mg}(\text{NO}_3)_2$. The samples were then dried, and calcined at 723K for 2 hours. The authors reported surface areas of 136-184 m^2/g depending on the % MgO. The catalyst was then added by impregnating the support in an ammonium hexamolybdate solution, and calcined again. The final catalyst was found to be very active and stable toward the oxidative dehydrogenation of propane, but was found to lose selectivity due to the formation of carbon oxides. More recently Chi, et al. published results of nitrates being adsorbed onto $\text{MgO}/\text{Al}_2\text{O}_3$. These results demonstrated that $\text{MgO}/\text{Al}_2\text{O}_3$ adsorbed more NO at 523K than did $\text{Tb}_4\text{O}_7/\text{Al}_2\text{O}_3$, $\text{La}_2\text{O}_3/\text{Al}_2\text{O}_3$, or $\text{BaO}/\text{Al}_2\text{O}_3$.

Whether alone or as a part of a mixed metal oxide, alumina or aluminum oxide (Al_2O_3) is probably the most important metal oxide, both for catalysis and in other applications such as an absorbent for organic molecules and as a wear-resistant coating. Because alumina has so many uses, there are a number of preparative methods available. Recently, significant interest has been expressed in NC alumina and the size-dependent properties thereof. Several researchers have undertaken projects to find improvements in alumina strength, catalytic activity and ductility, based upon decreasing the crystallite size.

In 1991 Chou, et al. published data on preparing nanocrystalline alumina via reactive sputtering deposition. Using this technique γ aluminum oxide films were deposited from a hot pressed Al_2O_3 target by r.f. magnetron reactive sputter deposition in a plasma of argon and oxygen. These films were deposited onto silicon and NaCl substrates, and were found to have

an average grain (crystallite) size of 10 nm, and after annealing at 800°C for 2 hours this remained constant. However, the grain size grew upon heating at 800°C for 24 hours, 1000°C for 2 hours, and 1200°C for 2 hours to 13 nm, 15 nm, and 50 nm respectively. This report yielded good insight into the micromechanical properties of nanocrystalline films. Later, Dockale, et al. reported on the enhanced surface reactivity of nanocrystalline alumina. In their work the nanocrystalline alumina was synthesized by gas phase condensation using a DC arc plasma technique. This technique produced 20–80 nm spherical polymorphous aluminum particles, which was highly crystalline according to XRD patterns. Also discussed was the enhanced surface activity of the alumina. An interesting method of preparation utilizing crysol techniques was reported by Mamchik, et al. An aluminum nitrate solution (in water) was first prepared and then sent through ion exchange using a polymeric base anion exchange resin to convert the $\text{Al}(\text{NO}_3)_3$ to $\text{Al}(\text{OH})_3$. Next the colloid was frozen and freeze dried to leave dry $\text{Al}(\text{OH})_3$. Lastly a step of thermal dehydration was used to convert the hydroxide to oxide. Although these authors discussed an interesting method of preparation, the characterization data, although showing that the sample was made up of amorphous γ and α alumina, was focused on ^{27}Al NMR.

In 1999 Patra, et al. published a preparation for alumina nanoparticles to be used for catalyst supports. In this work alumina was prepared by the hydrolysis of alumina sec-butoxide in 1-octanol, 1-butanol, and acetonitrile. In this method a dispersant (hydroxy propylcellulose) was used. The resulting alumina consisted of 200 nm particles, the crystal phase unknown. Later that same year Wang, et al. reported preparing nanocrystalline alumina by sol-gel methods. The crystallite size of the $\gamma\text{-Al}_2\text{O}_3$ was found after annealing at 400°C, 600°C, and 800°C to be 5.5 nm, 7.9 nm, and 9.7 nm respectively. More recently Ramesh, et al. studied the preparation of nanocrystalline $\gamma\text{-Al}_2\text{O}_3$ by hydrolysis of aluminum triisopropoxide, under ultrasound and in the presence of a peptizer. The dried samples were calcined at 700°C. The XRD patterns confirm that the samples were amorphous, and surface area before calcining were 83-143 m^2/g , and after calcining 97-183 m^2/g .

Despite the magnitude of prior efforts to produce small crystallite/high surface area alumina, a practical limit of 450-550 m^2/g BET surface area has never been exceeded. Given the commercial importance of alumina, a method for producing NC Al_2O_3 having significantly higher surface areas would be a signal development. By the same token, new NC mixed metal oxides

and hydroxides likewise having small crystallite size/high surface areas and enhanced surface chemistries would be highly desirable.

SUMMARY OF THE INVENTION

5 The present invention in one aspect is directed to the provision of particulate compositions comprising at least two nanocrystalline materials selected from the group consisting of the oxides and hydroxides of the elements of Groups IIA, IIIA, IVA, the transition metals and the lanthanide series of the Periodic Table, where at least one of the materials exhibits an average crystallite size of about 4 nm or less by XRD analysis. As used herein, reference to
10 an average crystallite size of about 4 nm or less embraces situations where, by XRD analysis, the analysis indicates no crystallite size whatsoever, or alternately a small crystallite size up to about 4 nm, i.e., the average crystallite size ranges from about zero to up to about 4nm. Such compositions also normally have a BET surface area which is at least about 30%, and more preferably at least about 50%, greater than the corresponding surface area of at least one of the
15 individual nanocrystalline materials, and more preferably each of such individual nanocrystalline materials, if the respective NC materials were prepared alone using the same conditions as the mixed compositions of the invention.

In preferred forms, the compositions are made up of from 2-4 different oxides or hydroxides, and most preferably are binary systems containing two different materials; moreover,
20 all of the different materials of the composition should advantageously have an average crystallite size of from about zero up to about 4 nm or by XRD analysis. The preferred class of different materials are selected from the group consisting of the oxides and hydroxides of Al, Mg, Ca, Sr, Ba, Zn, Co, Ni, Fe, Ti, Pd, Rh, V, Mn, Ga and Si. In the case of binary compositions the following combinations are especially desirable: $\text{Al}_2\text{O}_3 \cdot \text{MgO}$, $\text{Al}_2\text{O}_3 \cdot \text{CaO}$, $\text{Al}_2\text{O}_3 \cdot \text{SrO}$,
25 $\text{Al}_2\text{O}_3 \cdot \text{BaO}$, $\text{Al}_2\text{O}_3 \cdot \text{ZnO}$, $\text{Al}_2\text{O}_3 \cdot \text{CoO}$, $\text{Al}_2\text{O}_3 \cdot \text{NiO}$, $\text{Al}_2\text{O}_3 \cdot \text{Fe}_2\text{O}_3$, $\text{Al}_2\text{O}_3 \cdot \text{MgO} \cdot \text{TiO}_2$, $\text{Al}_2\text{O}_3 \cdot \text{PdO}$, $\text{Al}_2\text{O}_3 \cdot \text{RhO}$, $\text{Al}_2\text{O}_3 \cdot \text{V}_2\text{O}_3$, $\text{Al}_2\text{O}_3 \cdot \text{MnO}$, $\text{Ga}_2\text{O}_3 \cdot \text{MgO}$, and $\text{SiO}_2 \cdot \text{MgO}$. A particularly preferred binary composition contains aluminum oxide and magnesium oxide. Generally, one of the materials is present in a greater amount by weight as compared with another of the materials, so that the greater amount material can be deemed a matrix, with the lesser amount material being
30 dispersed within the matrix. In terms of molar ratios, binary compositions in accordance with

the invention should have a molar ratio of the first to the second material ranging from about 0.1-10.

The nanocrystalline compositions of the invention, made up of a plurality of nanocrystalline hydroxides or oxides, are fundamentally different than mere mixtures of two or more individually prepared hydroxides or oxides. That is, owing to the synthesis technique wherein the corresponding alkoxides are simultaneously co-solidified, the hydroxides or oxides of the final compositions are intimately intermingled on a molecular level. These compositions are not necessarily homogeneous, but in all cases the respective hydroxides or oxides making up the compositions are distributed on a molecular basis throughout the solidified compositions.

A method of preparing particulate, multiple nanocrystalline compositions comprises the steps of first separately preparing a plurality of different alkoxide solutions in respective compatible solvents, with each alkoxide including an ion moiety selected from the group consisting of the ions of the elements of Groups IIA, IIIA, IVA, the transition metals and the lanthanide series of the Periodic Table. These separate alkoxide solutions are mixed and hydrolyzed to yield an aqueous gel comprising the corresponding solidified hydroxides of the different alkoxides. Thereafter, the hydroxide gel is either dried to yield particulate hydroxide compositions or thermally converted to give the corresponding particulate oxide compositions.

Generally, each of the different alkoxides has the formula $[R-O]_n-X_q$, where R is a C1-C6 straight or branched chain alkyl group, X is an ion moiety as previously described, and n and q are selected so as to balance the valence of the alkoxide; particularly preferred alkoxides of this formula are those where R is a tert-butyl group.

In carrying out the synthesis of the mixed compositions to give oxide compositions, the thermal conversion step should be carried out at a temperature of from about 300-600°C for a period of from about 15-200 minutes. Of course, these conditions are variable, depending upon the nature of the selected starting materials. In the case of hydroxide compositions, the drying of the hydroxide gel is preferably carried out at a temperature of from about 25-300°C for a period of from about 15-200 minutes.

The mixed compositions of the invention are particularly useful for the sorption of target materials through adsorption or chemisorption. This involves contacting a selected composition with a target material under appropriate conditions. An almost limitless number of target

materials are subject to such treatment, such as those selected from the group consisting of compounds selected from the group of acids (e.g., H_2S and SO_2), alcohols (e.g., C1-C10 straight and branched chain organic alcohols), aldehydes, compounds containing an atom of P, S, N, Se, or Te, hydrocarbon compounds (e.g., halogenated hydrocarbons), toxic metal compounds, halogenated compounds, bacteria, fungi, viruses, rickettsiae, chlamydia, and toxins. One way of effecting contact between the compositions and target materials is contacting a fluid containing a target material with a quantity of the composition. The fluid may be a liquid or a gas (e.g., natural gas containing H_2S). Another method involves distributing a quantity of the composition onto an area where a target material is present, such as in environmental decontamination. The contacting can be carried out over a wide range of temperatures, typically from about -70-800°C, and more preferably from about -25-100°C.

The gel intermediates involved in the preferred synthesis of the composites are also a part of the invention, which as described can be dried to yield the hydroxides or converted to give the oxides.

In another aspect of the invention, nanocrystalline aluminum oxide is provided having extraordinarily high BET surface areas of at least about 700 m²/g and more preferably from about 725-850 m²/g. Such aluminas normally exhibit a completely amorphous pattern by XRD analysis. such aluminas can be used in the same fashion as the multiple-component compositions described above, i.e., the same classes of target materials, contacting techniques and temperatures are applicable.

BRIEF DESCRIPTION OF THE DRAWINGS

Figure 1 is a bar graph depicting the surface area results for nanocrystalline (NC- Al_2O_3) aluminum oxide produced in accordance with the present invention, after dynamic vacuum activation or argon flow activation;

Fig. 2 is a graph of the surface areas of CM- Al_2O_3 and NC- Al_2O_3 upon heat treatment;

Fig. 4 is a chart of XRD patterns for CM- Al_2O_3 and NC- Al_2O_3 ;

Fig. 3 is a graph of the surface area versus applied pressure on NC- Al_2O_3 (PL=pounds load);

Fig. 5 is a chart of XRD patterns of NC- Al_2O_3 after heating at 25°, 200°C, 400°C, 500°C, and 700°C;

Fig. 6a is a transmission electron microscope (TEM) photograph of CM-Al₂O₃

Fig. 6b is a TEM photograph of NC-Al₂O₃;

Fig. 7 is an high resolution TEM photograph of NC-Al₂O₃;

Fig. 8 a bar graph depicting the surface area results for aluminum/magnesium oxide after

5 dynamic vacuum activation or argon flow activation;

Fig. 9 is a graph of surface areas of CM-Al₂O₃, CM-MgO and NC-(1/1) Al₂O₃/MgO upon heat treatment;

Fig. 10 is a graph of surface area vs. applied pressure on NC-(1/1) Al₂O₃/MgO;

Fig. 11 is a chart of XRD patterns for CM-Al₂O₃, CM-MgO and NC-(1/1) Al₂O₃/MgO;

10 Fig. 12 is a chart of XRD patterns of NC-(1/1) Al₂O₃/MgO after heat treating at 25°, 100°C, 300°C, 500°C, and 700°C;

Fig. 13a is a TEM photograph of CM-MgO;

Fig. 13b is a TEM photograph of NC-Al₂O₃/MgO;

Fig. 14 is a graph illustrating the results of CCl₄ comparative destruction tests using CM-Al₂O₃ and NC-Al₂O₃;

Fig. 15 is a graph illustrating the results of CCl₄ comparative destruction tests using CM-Al₂O₃, CM-MgO, and NC-(1/1) Al₂O₃/MgO;

Fig. 16 is a schematic illustration of the IR cell used in SO₂ adsorption experiments in accordance with the invention;

20 Fig. 17 is a graph illustrating IR spectra after 2 hour evacuation at room temperature, for CM-Al₂O₃, NC-Al₂O₃, CM-MgO and NC-Al₂O₃/MgO;

Fig. 18 is a graph illustrating the results of a paraoxon sorption test using CM-Al₂O₃ and NC-Al₂O₃, showing paraoxon absorbance band versus time;

25 Fig. 19 is a graph illustrating the results of a paraoxon sorption test using CM-MgO, Al₂O₃/MgO and a blank, showing paraoxon absorbance band versus time; and

Fig. 20 is a graph illustrating IR spectra for CM-Al₂O₃, NC-Al₂O₃, CM-MgO, and NC-Al₂O₃/MgO taken after reaction with paraoxon.

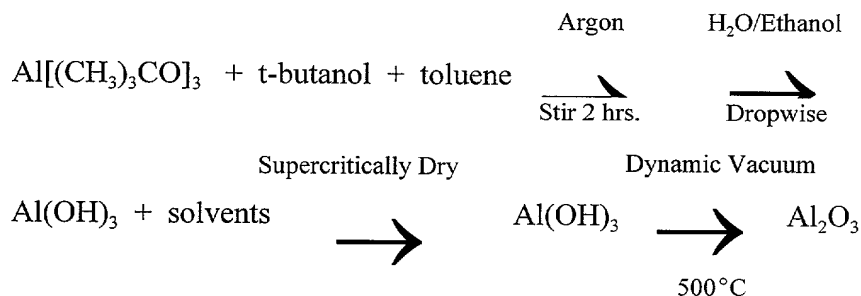
DETAILED DESCRIPTION OF THE PREFERRED EMBODIMENT

30 The following examples set forth preferred compositions and methods in accordance with the invention. It is to be understood, however, that these examples are provided by way of

illustration and nothing therein should be taken as a limitation upon the overall scope of the invention.

Preparation of Nanocrystalline (NC) Al_2O_3

In this example, pure nanocrystalline Al_2O_3 powder was synthesized and isolated. The reactions involved in the preparation are shown below.



The synthesis consisted of three main steps:

1. Synthesis of the aluminum hydroxide powder.

The chemicals used in the synthesis were directly from a commercial source without further purification. Under argon 1.00g (0.0040 mole) aluminum tri-*tert*-butoxide (Aldrich) was added to a 500 ml round bottom flask. The $Al[(CH_3)_3CO]_3$ was dissolved in a solution of 100 ml toluene (Fisher) and 40 ml *t*-butanol (Fisher) to form a clear colorless solution. A solution of 0.216 ml (0.0120 mole) distilled water in 70 ml absolute ethanol (Aaper Alcohol and Chemical Co.) was then added dropwise to the solution to form aluminum hydroxide gel. The reaction mixture was then stirred at room temperature for 10 hours. During this time the reaction mixture remained a clear colorless gel, but was dilute enough to maintain a liquid state.

2. Supercritical removal of the solvents.

The hydroxide sol-gel was transferred to a glass liner of a Parr autoclave. The autoclave was first flushed with nitrogen, and then (with nitrogen) pressurized to 100 PSI. The reactor was slowly heated ($1^\circ\text{C}/\text{min}$) with stirring from room temperature to 265°C . As the autoclave was heating, the pressure was increased from 100 PSI to 1100 PSI. Once the autoclave reached 265°C , the reactor was vented to the atmosphere very quickly removing the solvent vapors, (which took about 1 minute). Next, the furnace was removed and the bomb was flushed with nitrogen for 10 minutes to remove remaining solvent vapors. The autoclave was then allowed to cool to room temperature.

3. Thermal conversion of aluminum hydroxide to aluminum oxide.

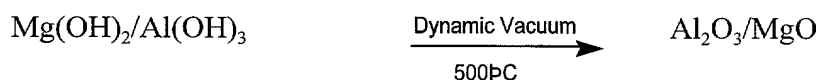
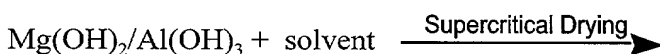
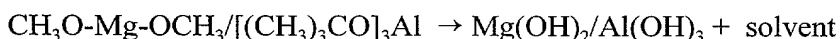
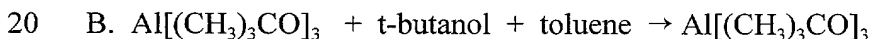
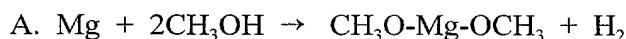
Data from thermogravimetric analysis (TGA) confirmed that the aluminum hydroxide to aluminum oxide conversion occurred between 400-450°C. The fluffy, white aluminum hydroxide powder was placed into a Schlenk tube, connected to a vacuum line and surrounded by a furnace.

- 5 The Schlenk tube was evacuated at room temperature for 1 hour. Next the Schlenk tube was slowly heated from room temperature to 500°C while under dynamic vacuum. After the heat treatment was complete the furnace was turned off and the Schlenk tube was allowed to cool to room temperature, still under dynamic vacuum. After heat treatment the aluminum oxide had a light gray color.

10

Preparation of Nanocrystalline (NC) Al₂O₃/MgO

In this example, the synthesis and isolation of nanocrystalline Al₂O₃/MgO powder was carried out, which involved first preparing an aluminum alkoxide solution, and a magnesium alkoxide solution. The two alkoxide solutions were then mixed in the desired molar ratio, and this solution was then allowed to react with a mixture of water in ethanol, and a hydroxide gel was formed. Upon solvent removal, a fine powder was obtained which was then heat treated under dynamic vacuum. The reactions involved in the preparation are shown below.



25

The preparation consisted of three main steps:

1. Synthesis of the aluminum/magnesium hydroxide gel.

The chemicals used in the synthesis were obtained from a commercial source without further purification. The magnesium methoxide solution was first prepared by adding 0.500g

(0.020 mole) of Mg (Fisher) (which had been sandpapered, wiped clean with an acetone wet kimwipe, and cut into small pieces) to a 200 ml round bottom flask under argon atmosphere. 50 ml methanol (Fisher) was added to the Mg, and this mixture was reacted and stirred overnight to form a clear colorless solution. 50 ml of toluene was then added to this solution, and the solution was stirred for 2 hours.

An aluminum tri-*tert*-butoxide solution was prepared by dissolving 1.00 g (0.0040 ml) aluminum tri-*tert*-butoxide (Aldrich) in 100 ml toluene (Fisher) and 40 ml *t*-butanol (Fisher) under an argon atmosphere in a 500 ml round bottom flask. A clear colorless solution was formed.

Lastly, the alkoxide solutions were mixed to give desired molar percentages, and then hydrolyzed. A solution containing a stoichiometric amount of distilled water in 70 ml absolute ethanol (Aaper Alcohol and Chemical Co.) was added dropwise to the alkoxide solutions to form the aluminum hydroxide/magnesium hydroxide gel. The reaction mixture was stirred at room temperature for 10 hours. During this time the reaction mixture remained a clear, colorless, liquid-like gel.

2. Supercritical removal of the solvents.

The hydroxide sol-gel was transferred to a glass liner of a Parr autoclave. The autoclave was first flushed with nitrogen, and the nitrogen was given an initial pressure of 100 PSI. While stirring, the reactor was slowly heated (1 °C/min) from room temperature to 265 °C. As the autoclave was heating, the pressure increased from 100 PSI to 1100 PSI. Once the autoclave reached 265 °C, the reactor was vented to the atmosphere very quickly removing the solvent vapors, which took about 1 minute. Next the furnace was removed and the bomb was flushed with nitrogen for 10 minutes to remove remaining solvent vapors. The autoclave was then allowed to cool to room temperature.

3. Thermal conversion of aluminum hydroxide/magnesium hydroxide to aluminum oxide/magnesium oxide.

Data from thermogravimetric analysis (TGA) confirmed that the hydroxide to oxide conversion occurred between 400-450 °C. The fluffy, white aluminum/magnesium hydroxide powder was placed into a Schlenk tube, connected to a vacuum line and surrounded by a furnace. The Schlenk tube was evacuated at room temperature for 1 hour. The tube then was slowly heated from room temperature to 500 °C while under dynamic vacuum. After the heat treatment

was complete, the furnace was turned off and the Schlenk was allowed to cool to room temperature, still under dynamic vacuum. After heat treatment, the aluminum/magnesium oxide had a light gray color.

Commercial aluminum oxide was purchased from Baker Analytical (CM-Al₂O₃) and commercial magnesium oxide was purchased from Aldrich (CM-MgO).

Characterization

(1) *Transmission electron microscopy (TEM)*. TEM studies were performed by adding dry ethanol to the heat-treated Al₂O₃ and sonicating this slurry for 5 minutes using a Branson 1210 sonicator. A drop of this slurry was then placed onto a carbon coated copper grid. The TEM experiments were performed using a Philips 201 TEM and a Philips CM12 TEM.

(2) *Brunauer-Emmet-Teller (BET)*. Surface area measurements were performed using BET methods. These measurements were conducted using both Micromeritics Flowsorb II 2300 and Quantachrome NOVA 1200 instrumentation. The samples were first outgassed at the desired temperature, and then allowed to cool to room temperature. Next they were further cooled to 77K and exposed to nitrogen/helium mixture (30% N₂, 70% He) where the adsorption of nitrogen molecules occurred. The amount of nitrogen adsorbed as a monolayer was measured. From the number of molecules adsorbed, and knowing the area occupied by each, the surface area was directly calculated.

(3) *Powder X-ray Diffraction (XRD)*. For XRD studies, the powder samples were heat treated under vacuum immediately before being placed onto the sample holder. The instrument used was a Scintag XDS 2000 spectrometer using CuK α radiation with 2 θ range of 20-85°, although an equivalent unit could be used. CuK α radiation was the light source used with applied voltage of 40 KV and current of 40 mA. The two theta angles ranged from 20° to 85° with a speed of 2° per minute. Spectra were run with a 0.02° step and a 0.08s step count with slit widths 2, 4 and 1, 05. The crystallite size was then calculated from the XRD spectra using the Debye-Scherrer equation by measuring the peak with a half maximum.

In particular, the sample was placed in a plastic sample plate having a depth of 2 nm. The powder was spread evenly over the sample plate, then pressed with a microscope slide to insure that the sample was flat and homogeneous. The sample plate was held in the instrument using a spring-loaded sample holder located between the X-ray gun and the detector. The sample was

then placed on the holder and the holder was allowed to rise gently until the sample place was clamped in position.

As used herein, "XRD analysis" refers to this procedure.

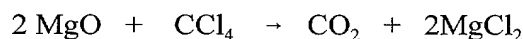
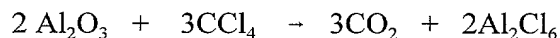
(4) *Infrared Spectroscopy* (FT-IR). FT-IR was used to observe solvent removal during the heat treatment process. These experiments were conducted on an RS-1 FTIR spectrometer from Mattson with a liquid nitrogen cooled MCT detector. Heat-treated samples of NC-Al₂O₃ and CM-Al₂O₃ were made into KBr pellets and studied.

(5) *Thermogravimetric Analysis* (TGA). TGA was used to determine the conversion of Al(OH)₃ to Al₂O₃ during heat treatment. These studies were conducted under a nitrogen flow. To measure the weight loss, the Al₂O₃ samples were placed onto a basket and heated at a rate of 10°/min from room temperature to 700°C. The instrument used was a thermogravimetric analyzer TGA-50 from the Shimadzu Company.

(6) *Elemental Analysis*. After heat treatment, the Al₂O₃ was transferred to glass vials, placed under argon atmosphere, and analyzed for Al, C, and H. The amount of oxygen was obtained by subtracting the sum of Al, C, and H from 100.

Adsorption Studies

1. Reaction of Al₂O₃, and Al₂O₃/MgO with CCl₄



The chemical reactivity of the metal oxides was determined by reacting the metal oxides with CCl₄. The reactions were conducted in a U-tube that was connected to a gas chromatograph (GOW-MAC gas chromatograph series 580). The U-tube was made of Pyrex and connected between the injector port and the column (Alltech Chromosorb W-HP). An oxide sample (0.100 gram) was placed in the U-tube between two small plugs of quartz wool. The U-tube was heated to 500°C and the injector port was kept at 100 °C. 2μl of CCl₄ were injected every seven minutes. Any CO₂ coming off the sample, or CCl₄ that was not destroyed, was then sent via helium (20cc/min) through the column (90 °C) to be separated. Any CO₂ or CCl₄ was detected by a thermal conductivity detector (120 °C) and peak areas recorded. Injections of CCl₄ were made until the oxide bed had been exhausted.

2 Sulfur Dioxide Adsorption

A quartz spring balance was used to measure the adsorption of SO_2 onto Al_2O_3 and $\text{Al}_2\text{O}_3/\text{MgO}$. The apparatus consisted of a basket used to hold the sample and was attached to a quartz spring. The basket and the spring were closed within the vacuum line. The SO_2 gas tank was also attached to the vacuum line. As the SO_2 adsorbed onto the metal oxide in the basket, the weight change caused the spring to move, and this movement was noted by the telescope. Once calibrated, the telescope was accurate to ± 0.1 mg.

Due to the electrostatic properties of the fine powders, it was found to be much easier and more accurate to work with granules. Using granules helped to eliminate losses during transfers, weighing, and applying vacuum. Therefore, the samples were first pressed into pellets at 1000 pounds load, then crushed and sifted through a mesh to achieve granules having a size of about 0.250 mm to 1.17mm. By using a relatively low pelletization pressure, only a small change in surface area resulted.

Granules (100 mg) of oxides were placed into the basket on the spring balance. The samples were placed under dynamic vacuum for 1 hour at room temperature. After evacuation, the vacuum line was closed to the pump and the spring position was noted. The vacuum line including the spring balance was filled with SO_2 gas to the desired pressure. The spring position was noted over the next hour. The vacuum line was then evacuated for 100 minutes to remove all physisorbed species. After the evacuation, the spring position, which indicated the presence of remaining strongly chemisorbed species was noted again.

3. Destructive Adsorption of Diethyl 4-Nitrophenyl Phosphate

In this example, the destructive adsorption of diethyl 4-nitrophenyl phosphate (DNPP, also called paraoxon) and considered a chemical warfare mimic), was carried out to determine the capacity of the oxide to dissociatively chemisorb a polar organophosphorous compound. A 0.100 g sample was placed into a 250 ml round bottom flask that had been flushed with argon. 100 ml dry pentane was then added to the flask, and the mixture was stirred. 8 μl paraoxon was added to the flask. By extracting samples at desired intervals, ultraviolet/visible spectroscopy (SIM Aminco Milton Roy 3000 array) was used to monitor the disappearance of paraoxon at 270 nm wavelength, by extracting samples at desired intervals. The destructive adsorption reaction was monitored every 20 minutes for the first 3 hours, and then again at 20 hours. The powder was filtered and FTIR was used to detect adsorbed species on the solid. The used solid was then

washed with 10 ml portions of CH_2Cl_2 , IR analysis of the extracted CH_2Cl_2 showed that no adsorbed species were removed.

Preparation of the Aluminum Oxide

- 5 Several experiments were conducted using various the starting materials, solvents, and stirring times; all of which were found to have an effect on the surface area of the resulting sample. Results are shown in Table 1.

Table 1. Aluminum Oxide Preparation Variables

Sample #	Starting Material	Solvent	Stirring Time	Surface Area (m^2/g)
1	Aluminum Triethoxide	Toluene/Ethanol (100ml/40 ml)	2 hr	352
2	Aluminum Triethoxide	Toluene/Ethanol (100ml/40 ml)	10 hr	385
3	Aluminum Isopropoxide	Toluene/Isopropanol (100ml/40ml)	2 hr	224
4	Aluminum Isopropoxide	Toluene/Isopropanol (100ml/40ml)	10 hr	243
5	Aluminum Tributoxide	Toluene/Butanol (100ml/40ml)	2 hr	392
6	Aluminum Tributoxide	Toluene/Butanol (100ml/40ml)	10 hr	369
7	Aluminum Tri- <i>tert</i> -butoxide	Toluene/ <i>t</i> -Butanol (100ml/40ml)	2 hr	743
8	Aluminum Tri- <i>tert</i> -butoxide	Toluene/ <i>t</i> -Butanol (100ml/40ml)	10 hr	810
9	Aluminum Tri- <i>tert</i> -butoxide	Toluene/ <i>t</i> -Butanol (100ml/40ml)	20 hr	735
10	Aluminum Tri- <i>tert</i> -butoxide	Toluene/ <i>t</i> -Butanol (50ml/40ml)	10 hr	673
11	Aluminum Tri- <i>tert</i> -butoxide	Toluene/ <i>t</i> -Butanol (150ml/40ml)	10 hr	779

Sample #8, using aluminum tri-*tert*-butoxide as the starting material exhibited the highest surface area. Stirring time was found to be a relevant factor in determining surface area. Enough time had to be allowed for hydrolysis to occur, but too much stirring time resulted in lower surface areas. The amount of solvent used was also studied and found to have a role in the surface area. In samples 8, 10, and 11 it was found that decreasing the amount of toluene from 100 ml to 50 ml resulted in a significant decrease in surface area, going from 786 to 673 m²/g. When the amount of solvent was increased from 100 ml to 150 ml as in samples 10, and 11, the surface area only slightly decreased from 786 to 779 m²/g.

Activation of the Aluminum Oxide (Thermal Dehydration)

In this experiment, aluminum oxide was activated under either argon flow, or dynamic vacuum. The Al₂O₃ surface areas for each method of activities are shown in Fig. 1. The Al₂O₃ surface area is significantly higher for the sample activated under dynamic vacuum then argon flow. Generally, during activation, the surface area increases, then goes through a maximum, and then decreases. The small decrease in surface area at temperatures above 400°C can be explained by sintering.

Aluminum Oxide Characterization.

Through careful characterization of the Al₂O₃ samples, it was discovered that the NC-Al₂O₃ samples had morphology different from that of the commercial (CM) Al₂O₃ samples.

(1) *Brunauer-Emmet-Teller Method (BET).* Commercial Al₂O₃ is most commonly prepared by high temperature methods, and has surface areas within the range of 100 – 110 m²/g. The NC- Al₂O₃ samples typically possessed surface areas within the range of 790-810 m²/g after heat treatment at 500°C. When heated at higher temperatures the crystallites began to sinter, and surface areas decreased. Fig. 2 shows the heat treatment temperature dependence observed in NC-Al₂O₃ compared to CM-Al₂O₃.

Using BET, data on the Al₂O₃ pore structures was obtained. The average NC- Al₂O₃ sample after heat treatment possessed pores that were 10 nm in diameter, held 2.05 cc/g volume, and had a cylindrical pore structure that was open at both ends. See Table 2.

Table 2. Surface area, pore volume and diameter of CM-Al₂O₃ and NC- Al₂O₃.

Sample	Surface Area	Average Pore Volume	Average Pore Diameter
CM-Al ₂ O ₃	103 m ² /g	0.19 cc/g	7.4 nm
NC-Al ₂ O ₃	805 m ² /g	2.1 cc/g	11 nm

Pellets of the NC-Al₂O₃ were prepared and heat treated at 500°C. Pellets were pressed under various pressures and then studied by BET methods to measure the effects of pressure surface area, pore diameter, pore volume, and pore shape. The pressures tested in pounds load (PL) were 2000 PL, 5000 PL, 10,000 PL, and 20,000 PL. Fig. 3 shows how the surface area varied with pressure. Before being pressed, the samples had about 800 m²/g surface area. When pressed at 2000 PL, the surface area fell to 752 m²/g, and fell to 486 m²/g at 20,000 PL. The pore diameter also changed with increasing pressure. When not pressed, the samples have 10.8 nm pore openings. Under 2000 PL, the pore openings decreased slightly to 10.7 nm and then dropped to 7 nm at 20,000 PL. Pore volume also changed with pressure, but not as drastically as the average pore diameter. Before being pressed, the samples had 2.05 cc/g volume, and after being pressed at 2000 PL, the volume dropped slightly to 1.85 cc/g. However, after being pressed at 10,000 PL, the volume decreased to 1.22 cc/g and remained at that level even after being pressed at 20,000 PL. Table 3 shows how the pore shape of the NC-Al₂O₃ sample changed with increasing pressure, according to De Boer's hysteresis.

Table 3. Pressure and resulting pore shape for NC-Al₂O₃.

Pressure (PL)	Pore Shape
0 PL	Cylindrical Pores Open at Both Ends
2,000 PL	Cylindrical Pores Open at Both Ends
5,000 PL	Cylindrical Pores Open at Both Ends
10,000 PL	Cylindrical Pores Open at Both Ends
20,000 PL	Tapered or Wedged Shaped Pores with Narrow Necks, Open at One or Both Ends

Before any pressure was applied, the sample had a pore structure consisting of cylindrical pores open at both ends. When pressure was applied, this pore structure remained, until when, at 20,000 PL, it was replaced with slit shaped pores, the space between parallel plates.

(2) *X-ray Diffraction (XRD)*. From XRD, diffraction patterns that showed the NC-
5 Al_2O_3 sample to be less crystalline than the commercial Al_2O_3 samples. The NC- Al_2O_3 had a completely amorphous pattern (Fig. 4) due to particle size broadening which occurs when a sample is made up of very small crystallites. Using the Scherrer equation, the crystallites size may be calculated based on the broadness of the peaks.

Even as the temperature was increased, the crystallite size of NC- Al_2O_3 was not able to
10 be determined from the diffraction patterns. The data showed that the NC- Al_2O_3 had a significantly smaller crystallite size than the commercial Al_2O_3 samples. The average crystallite size for NC- Al_2O_3 activated at 500°C was less than 2 nm, while the average crystallite size for CM- Al_2O_3 was 19 nm. Fig. 5 shows the x-ray diffraction patterns of NC- Al_2O_3 heated from 25°C to 700°C . The conversion of $\text{Al}(\text{OH})_3$, could not be determined by viewing the XRD patterns.
5

(3) *Infrared Spectroscopy (IR)*. IR was used to study the aluminum oxide powder during heat activation. The heat-treated samples were ground with KBr, and pressed into pellets. IR spectra were taken after heat treatment at 25°C , 50°C , 100°C , 150°C , 200°C , 250°C , 300°C , 400°C and 500°C . A gradual loss of water, and solvent could be seen from 25°C to 500°C . Even
20 after 500°C heat treatment, some residual $-\text{OH}$ groups remained.

(4) *Thermogravimetric Analysis (TGA)*. Using TGA, weight loss under nitrogen flow was observed to be about 35%. The weight loss was found to be the same when conducted in air. One major weight loss occurs between 420°C to 460°C , and was due to the conversion of $\text{Al}(\text{OH})_3$ to Al_2O_3 , and the removal of the water. Theoretically, the conversion of $\text{Al}(\text{OH})_3$ to
25 Al_2O_3 should yield a 35% weight loss, whereas the weight loss would be 23% if the $\text{Al}(\text{OH})_3$ were converted to AlOOH .

(5) *Transmission Electron Microscope (TEM)*. Figs. 6a and 6b show TEM photographs of CM- Al_2O_3 and NC- Al_2O_3 respectively. The CM- Al_2O_3 sample (Fig. 6a) appeared as a grainy material with crystallites greater than 10 nm. The NC- Al_2O_3 sample (Fig.
30 6b) consisted of crystallites having an average crystallite size of about 5 nm, but of a different morphology. By compiling data from XRD, TEM, and BET, it was concluded that the NC-

Al_2O_3 samples are made up of crystallites having an average size of less than 2 nm. The NC- Al_2O_3 sample was further investigated using HRTEM which confirmed that the average crystallite size was less than 2 nm, and disordered (Fig. 7).

(6) *Elemental Analysis.* Table 4 shows the elemental analysis results of NC- Al_2O_3 that was preheat-treated to 500 °C under dynamic vacuum. These data indicated the presence of some residual OH/ H_2O . IR analysis indicated the presence of adsorbed CO_2 . If CO_2 and surface OH are assumed to be the only adsorbed species, a formula $\text{Al}_2\text{O}_{2.7}(\text{OH})_{0.53}(\text{CO}_2)_{0.03}$ fits the data (oxygen by difference).

Table 4: Elemental analysis for NC- Al_2O_3

Element	% Calculated	% Experimental
Aluminum	52.9%	47.1%
Oxygen	47.1%	51.9%
Carbon	0%	< 0.50%
Hydrogen	0%	< 0.50%

Preparation of the Aluminum/Magnesium Oxide

In this experiment, the quantity of solvent, stirring time, and molar ratios were varied. all of the variables were found to have an effect on the surface area of the resulting sample. Some of the results are shown in Table 5.

Table 5: Aluminum/Magnesium Oxide Preparation Variables

Sample #	Molar Ratio $\text{Al}_2\text{O}_3/\text{MgO}$	Solvent ml	Stirring Time	Surface Area (m^2/g)
1	1/1	20 ml	1 hr	559
2	1/1	70 ml	1 hr	762
3	1/1	120 ml	1 hr	743
4	1/1	70 ml	10 hr	815
5	1/1	70 ml	20 hr	796
6	1/2	70 ml	10 hr	775
7	2/1	70 ml	10 hr	834

Sample number seven, using a 2:1 Al_2O_3 to MgO ratio, produced $\text{Al}_2\text{O}_3/\text{MgO}$ having the highest surface area. For 1:1 Al_2O_3 to MgO samples, stirring time was found to be a factor in determining surface area. Sufficient stirring time was needed for hydrolysis to occur, but too much stirring time resulted in lower surface areas. The amount of solvent (ethanol) used in the hydrolysis step was also studied and found to have an important role in the surface area. Decreasing the amount of ethanol from 70 ml to 20 ml as in samples 1 and 2, resulted in a significant decrease in surface area, going from 762 to 559 m^2/g . When increasing the amount of solvent from 70-170 ml as in samples 2, and 3, the surface area decreased from 762 to 743 m^2/g .

Activation of the Aluminum/Magnesium Oxide (Thermal Dehydration)

Aluminum/magnesium oxide was activated under either argon flow or dynamic vacuum. The surface areas produced for each activation method are shown in Fig. 8. The particle surface area is slightly higher for the sample activated under dynamic vacuum than those activated under argon flow. Generally, during activation the surface area increased, then went through a maximum, and then decreased. The small decrease in surface area at temperatures above 400 °C can be explained by sintering.

(1/1) Aluminum Oxide Magnesium Oxide Characterization

Careful characterization of the (1/1) (Molar Ratio) $\text{Al}_2\text{O}_3/\text{MgO}$ samples demonstrated that the NC- $\text{Al}_2\text{O}_3/\text{MgO}$ samples had morphology different from that of the commercial (CM) Al_2O_3 and MgO samples.

(1) *Brunauer-Emmet-Teller Method (BET)*. The NC- (1/1) $\text{Al}_2\text{O}_3/\text{MgO}$ samples which were heat treated at 500 °C typically possessed surface areas within the range of 770-810 m^2/g . When heated at higher temperatures, the crystallites began to sinter, and as a result, the surface areas decreased. Fig. 9 shows the heat treatment temperature dependence observed in NC-(1/1) $\text{Al}_2\text{O}_3/\text{MgO}$ compared to CM- Al_2O_3 and CM-MgO.

Using BET, pore structure data was obtained. The average NC-(1/1) $\text{Al}_2\text{O}_3/\text{MgO}$ sample after heat treatment possessed pores that were 10 nm in diameter, had a volume of 1.90 cc/g and had a cylindrical pore structure that was open at both ends.

In addition, NC SrO, Sr(OH)₂, mixed Mg/Sr, Al/Sr and tertiary Al/Mg/Sr materials were prepared by the same techniques described above for the Al₂O₃/MgO systems, except that the appropriate Sr reagents were employed. Table 6 below gives data characterizing the foregoing compositions, together with data for corresponding CM materials.

Table 6. Surface area, pore volume and diameter of nanocrystalline samples compared to commercially available samples.

Sample	Surface Area (m ² /g)	Average Pore Volume (cc/g)	Average Pore Diameter (nm)
CM-Al ₂ O ₃	103	0.19	7.4
CM-MgO	18.7	0.077	16
NC-Al ₂ O ₃	805	2.1	11
NC-Al ₂ O ₃ /MgO ^b	793	1.9	11
NC-MgO ^a	400	0.90	9.0
CM-SrO	1.1	0.0055	19
NC-SrO	19	0.06	13
CM-Sr(OH) ₂	4.0	0.0083	8.2
NC-Sr(OH) ₂	8.1	0.0076	27
NC-Mg(OH) ₂ /Sr(OH) ₂	180	0.5	11
NC-Mg(OH) ₂	460	1.6	9.0
NC-MgO/SrO	135	0.38	11
NC-Al(OH) ₃ /Sr(OH) ₂	175	--	--
NC-Al ₂ O ₃ /SrO	137	0.52	15
NC-Al ₂ O ₃ /MgO/SrO	195	0.51	11
NC-Al(OH) ₃ /Mg(OH) ₂ /Sr(OH) ₂	225	0.54	9.8

(a) Also referred to as AP-MgO for aerogel prepared.

(b) One mole Al₂O₃ to one mole MgO.

Pellets of the NC-(1/1) Al₂O₃/MgO heat treated at 500°C were prepared. The pellets were pressed at various pressures and then studied by BET methods to determine the effect of pressure

on surface area, pore diameter, pore volume, and pore shape. The pressures tested in pounds load (PL) were 2,000 PL, 5,000 PL, 10,000 PL, and 20,000 PL. Fig. 10 shows how the surface area varied with pressure. The unpressed samples had surface areas of 772 m²/g when pressed at 2,000 PL and the surface area fell to 547 m²/g, and at 20,000 PL, the surface area fell to 502 m²/g.

The pore diameter was also affected by pressure. The unpressed samples had 10.8 nm pores which decreased to 7.76 nm at 2000 PL, and then dropped to 6 nm at 20,000 PL. Pore volume also changed with pressure, but not as drastically as the diameter or the surface area. The unpressed samples had 1.90 cc/g volume, and after being pressed at 2000 PL the volume dropped to 0.742 cc/g, at 10,000 PL, the volume decreased to 0.635 cc/g and remained at that level even after being pressed at 20,000 PL. Table 7 shows how the pore shape of the NC-Al₂O₃/MgO sample changed with increasing pressure, according to De Boer's hysteresis.

Table 7: Pressure and resulting pore shape for NC-Al₂O₃/MgO.

Pressure (PL)	Pore Shape
0 PL	Cylindrical Pores Open at Both Ends
2,000 PL	Cylindrical Pores Open at Both Ends
5,000 PL	Cylindrical Pores Open at Both Ends
10,000 PL	Tapered or Wedged Shaped Pores with Narrow Necks, Open at One or Both Ends
20,000 PL	Tapered or Wedged Shaped Pores with Narrow Necks, Open at One or Both Ends

Before any pressure was applied, the sample had a pore structure consisting of cylindrical pores open at both ends. This pore structure remained until 10,000 PL, where the cylindrical pores were transformed into tapered or wedged shaped pores with narrow necks, open at one or both ends.

(2) *X-ray Diffraction.* XRD diffraction patterns were obtained that showed the NC-Al₂O₃/MgO sample to be less crystalline than the commercial MgO and Al₂O₃ samples. The NC-Al₂O₃/MgO had a completely amorphous pattern (Fig. 11), due to severe particle size broadening.

The crystallite size of NC-(1) Al₂O₃/MgO could not be determined from the diffraction patterns, even as the temperature was increased. The results show that the NC-Al₂O₃/MgO has a significantly smaller crystallite size than the commercial MgO and Al₂O₃ samples. The average

crystallite size for NC- $\text{Al}_2\text{O}_3/\text{MgO}$ activated at 500°C was 2 nm or less, whereas the average crystallite size for CM-MgO was 87 nm, and for CM- Al_2O_3 , 19 nm. Fig. 12 shows the XRD patterns of NC- $\text{Al}_2\text{O}_3/\text{MgO}$ heated from 25° to 700°C . The conversion of the hydroxide to oxide, could not be determined from the XRD patterns.

(3) *Infrared Spectroscopy.* IR was used to study the aluminum oxide powder during heat activation. The heat-treated samples were ground with KBr, and pressed into pellets. IR spectra were taken after heat treatment of the pellets at 25°C , 100°C , 200°C , 300°C , 400°C and 500°C . A gradual loss of water, and solvent was observed from 25°C to 500°C . Therefore, when activating the Al_2O_3 at 500°C , a small amount of residual surface $-\text{OH}$ will be present.

(4) *Thermogravimetric Analysis.* Particle weight loss under nitrogen flow was found to be about 40%. Similar results were observed with TGA conducted in air. The gradual weight loss observed throughout the heating was due to the hydroxide converting to oxide, and the removal of the water. The theoretical weight loss is 34%, so the observed 40% indicated that some adsorbed water was also present.

(5) *Transmission Electron Microscope.* TEM was also used to evaluate NC- $\text{Al}_2\text{O}_3/\text{MgO}$, CM-MgO and CM- Al_2O_3 samples. Figs. 13a, b, and c show the respective TEM photographs. The CM-MgO sample consisted of single crystals having an estimated crystallite size of 10 nm (Fig. 6a). The CM-MgO sample consisted of single crystals having an estimated crystallite size of 82 nm (Fig. 13a). The NC- $\text{Al}_2\text{O}_3/\text{MgO}$ sample (Fig. 13b) however consisted of crystallites having an average crystallite size of about 5 nm or smaller according to TEM. By compiling data from XRD, TEM, and BET it was determined that the NC-(1/1) $\text{Al}_2\text{O}_3/\text{MgO}$ samples are made up of $\leq 2\text{nm}$ crystallites.

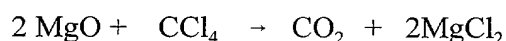
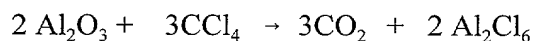
(6) *Elemental Analysis.* Table 8 shows the elemental analysis results of NC-(1/1) $\text{Al}_2\text{O}_3/\text{MgO}$ preheat-treated to 500°C under dynamic vacuum. The data indicated the presence of some residual OH/ H_2O adsorbed CO_2 was further indicated by IR. Assuming that CO_2 and surface H_2O are the only adsorbed species, a formula $\text{Al}_2\text{O}_3 \cdot \text{MgO} (\text{OH})_{1.4} (\text{CO}_2)_{0.088} (\text{H}_2\text{O})_{0.35}$ fits the data (oxygen by difference).

Table 8: Elemental analysis for NC-(1/1) Al₂O₃/MgO

Element	% Calculated	% Experimental
Magnesium	17%	13.3%
Aluminum	37.9%	30.9
Oxygen	45.0%	53.9%
Carbon	0%	< 0.65%
Hydrogen	0%	< 1.20%

Adsorption Studies

Reaction of Al₂O₃ and (1/1) Al₂O₃/MgO with CCl₄. In this example, Al₂O₃ and Al₂O₃/MgO was reacted with CCl₄ to determine the destructive adsorption abilities of the metal oxides toward a model chlorocarbon at elevated adsorption temperatures.



Based strictly on thermodynamic properties, the samples should be more reactive than the Al₂O₃ samples. However, as shown below, surface area, crystallite size, and morphology contribute to reactivity.

The above reactions were conducted via the pulse method and the products were identified by GC. The breakthrough injection, saturation injection, and molar ratios are reported in Table 9. The breakthrough injection of the reaction is the first injection that a complete destruction of CCl₄ does not occur as sensed by the detector. The saturation injection is the first injection that 100% of the injected CCl₄ is measured by the GC detector.

Table 9: Reaction of pulses of CCl_4 with oxide samples

Sample	Breakthrough	Saturation	Molar Ratio
NC- Al_2O_3	57	98	1.44 mole CCl_4 : 1 mole Al_2O_3
CM- Al_2O_3	2	17	1 mole CCl_4 : 16 mole Al_2O_3
NC-(1/1) $\text{Al}_2\text{O}_3/\text{MgO}$	25	88	1.8 mole CCl_4 :1 mole
CM-MgO	1	14	1 mole CCl_4 : 32 mole MgO

Theoretical Molar Ratios: 1 mole CCl_4 :2 mole MgO
 1.5 mole CCl_4 :1 mole Al_2O_3
 2 mole CCl_4 :1 mole $\text{Al}_2\text{O}_3/\text{MgO}$

CCl_4 Adsorption. Figs. 14-15 show graphs of the percent CCl_4 destroyed vs. the injection number. The CM- Al_2O_3 sample showed breakthrough at the second injection, and was saturated by the 17th injection. The NC- Al_2O_3 samples showed breakthrough on the 58th injection, and were saturated on the 98th injection. The CM-MgO samples showed breakthrough at the first injection, and were saturated by the 14th injection. The NC-(1/1) $\text{Al}_2\text{O}_3/\text{MgO}$ samples exhibited much higher saturation numbers, destroying 100% of the injected CCl_4 for the first 25 injections. The NC-(1/1) $\text{Al}_2\text{O}_3/\text{MgO}$ samples partially reacted with CCl_4 until the 88th injection where saturation occurred. The theoretical molar ratio of $\text{MgO}:\text{CCl}_4$ of the solution is 1:1.5, and (1/1) $\text{Al}_2\text{O}_3/\text{MgO}:\text{CCl}_4$ is 1:2. The data results showed that the NC samples were much more reactive than the CM samples. The experimental molar ratio of NC- $\text{Al}_2\text{O}_3:\text{CCl}_4$ at saturation sample was 1:1.44, whereas the experimental molar ratio for CM- Al_2O_3 was 16:1. The data also showed that the NC- $\text{Al}_2\text{O}_3/\text{MgO}$ samples were much more reactive than the CM-MgO. The experimental molar ratio for NC- $\text{Al}_2\text{O}_3/\text{MgO}:\text{CCl}_4$ at saturation was 1:1.8, whereas the molar ratios for CM-MgO: CCl_4 samples was much higher.

Sulfur Dioxide Adsorption on Alumina, and Aluminum/Magnesium Oxide. In this example, adsorption of SO_2 was carried out to determine if the adsorption properties were different for nanocrystals compared to commercial microcrystals. These adsorption reactions were carried out on the quartz spring balance. The amount of SO_2 required for a monolayer of gas as the particle was calculated. Using 19.2 \AA^2 as the area of an SO_2 molecule, it was determined that 5.2 molecules SO_2/nm^2 would form a monolayer. The data showed that at atmospheric pressure and room temperature, up to 3.5 molecules SO_2/nm^2 adsorbed onto NC-

Al₂O₃. Similarly onto CM-Al₂O₃, 3.5 molecules SO₂/nm² adsorbed. However, 6.8 molecules SO₂/nm² adsorbed onto NC-(1/1) Al₂O₃/MgO whereas only 0.68 molecules SO₂/nm² adsorbed onto CM-MgO. See Table 10.

5 Table 10: Adsorption of SO₂ on Al₂O₃, MgO, and Al₂O₃/MgO samples at room temperature.

Sample	Total Molecules SO ₂ /nm ² Adsorbed	Molecules SO ₂ /nm ² Physisorbed	Molecules SO ₂ /nm ² Chemisorbed
NC-Al ₂ O ₃	3.5	1.8	1.7
CM-Al ₂ O ₃	3.5	3.0	0.45
NC-Al ₂ O ₃ /MgO	6.8	2.9	3.9
CM-MgO	0.68	0.51	0.17

10 The data indicate that NC-Al₂O₃/MgO efficiently adsorbed SO₂ in slightly more than one layer. After adsorption had ceased the samples were subjected to dynamic vacuum for 100 minutes to remove the physisorbed species. After this vacuum treatment, there remained 1.70 and 0.45 molecules SO₂/nm² chemisorbed onto the NC- Al₂O₃ and CM- Al₂O₃ samples respectively. The vacuum treatment removed most of the adsorbed SO₂ from the CM-MgO, whereas the NC- Al₂O₃/MgO sample retained 3.9 molecules SO₂/nm².

20 An *in situ* IR study was performed to help identify how the SO₂ was binding to the particles. Fig. 16 is a schematic of the IR cell used. Through this setup, the IR spectra of the same spot on the particle before SO₂ adsorption, with SO₂ adsorbed thereon, and after evacuation of SO₂ was obtained. The study was conducted at room temperature with 20 torr SO₂. The sample was placed on a tungsten mesh which was then placed into the cell, and the cell was then evacuated. Once optimum placement of the sample in the cell was found, background spectra
25 were collected. The cell was pressurized with 20 torr of SO₂ for 2 hours. The cell was then evacuated, and spectra were taken over the next 2 hours. Fig. 17 shows the spectra after 2 hour evacuation for all four samples. Both CM-MgO and CM-Al₂O₃ showed no adsorbed species. Both NC-Al₂O₃ and NC- Al₂O₃/MgO showed new peaks at 1466 cm⁻¹, which corresponding to chemisorbed monodentate SO₂ adsorbed species. The data indicated that the NC samples have
30 a high capacity for chemisorption of SO₂ (Table 10) per unit surface area indicating an intrinsically higher activity.

Destructive Adsorption of Diethyl 4-Nitrophenyl Phosphate (Paraoxon). In this example, the adsorption of paraoxon was carried out to compare the rates and capacities for the metal oxide samples to dissociatively chemisorb a polar organic species, and more specifically, a toxic insecticide. By monitoring the disappearance of an UV band for paraoxon in pentane the data shown in Table 11 and Figs. 18-19 were obtained.

Table 11: Destructive adsorption of Paraoxon in pentane on the oxide powders.

Sample	Molar Ratio
NC-Al ₂ O ₃	1 mole Paraoxon: 11 mole Al ₂ O ₃
CM-Al ₂ O ₃	1 mole Paraoxon: 63 mole Al ₂ O ₃
NC-(1/1)Al ₂ O ₃ /MgO	1 mole Paraoxon: 5.6 mole Al ₂ O ₃ /MgO
CM-MgO	1 mole Paraoxon: 188 mole MgO

Neither of the CM samples adsorbed much paraoxon, while the NC samples rapidly adsorbed the entire sample and developed a bright yellow color, indicating the likely formation of the p-nitrophenoxide anion on the surface.

Additional experiments with larger amounts of paraoxon were also carried out. It was found that about 5.5μl of paraoxon (2.55E-5 moles, 1.54E19 molecules) was adsorbed by 0.0300g NC-Al₂O₃, and about 9.5μl of liquid paraoxon (4.40E-5 moles, 2.65E19 molecules) was adsorbed by 0.0350g of NC-Al₂O₃/MgO. One molecule of dissociated paraoxon and with the p-nitrophenoxide group lying flat would occupy about 1 nm² of surface area. 2.4 E19 nm² surface area is available in a 0.0300g sample of NC- Al₂O₃. It is estimated that about 0.77 monolayer of paraoxon is adsorbed. 2.8 E19 nm² surface area is available in a 0.0350g sample of NC- Al₂O₃/MgO. It is estimated that about 1.04 monolayers are adsorbed under these conditions (room temperature, 0.01 M concentration in pentane).

After the reaction was complete the powders were filtered and IR studies were done on the materials. The data from the IR shows that the NC samples have many new species adsorbed to the powder, whereas the CM samples have little if any new species adsorbed. Table 12 gives IR spectra assignments for free paraoxon and for adsorbed paraoxon.

Table 12: FTIR bands for free paraoxon, and adsorbed paraoxon.

Free Paraoxon	Assignment	Adsorbed Paraoxon	Assignment
860	ν C-N	860	ν C-N
930	CH ₃ rock	930	CH ₃ rock
1045	ν Et-O-(P)	1045	ν C-O-(P)
1107	CH ₃ rock	1107	CH ₃ rock
1164	CH ₃ rock	1164	CH ₃ rock
1232	ν P-O-(Ar)		
1296	ν P=O	1313	ν P=O
1348	ν_s N-O	1348	ν_s N-O
1491	ν C-C ring	1491	ν C-C ring
1526	ν_{as} N-O	1526	
1593	ν C-C ring	1593	ν C-C ring

Fig. 20 shows the IR spectra for CM-Al₂O₃, NC-Al₂O₃, CM-MgO, and NC-(1/1) Al₂O₃/MgO taken following the reaction with paraoxon. There appears to be a change in the FTIR when paraoxon is adsorbed. A band at 1296 cm⁻¹ assigned to ν P=O is broadened and shifted to approximately 1313 cm⁻¹. Also, the original peak for free paraoxon at 1232 cm⁻¹ assigned to ν P-O-Ar stretch has dissapeared. The band due to ν P-O-Et at 1045 cm⁻¹ does not change much (see Table 12), suggesting that the EtO-P moieties are not perturbed or destroyed. These data demonstrate that P=O bond is strongly perturbed through binding to Lewis acid sites on the Al₂O₃ and MgO surfaces, and that the P-OAr bond is broken.